ARTICLES

Optical and Chemical Observations on Gold−Mercury Nanoparticles in Aqueous Solution

Arnim Henglein*

Radiation Laboratory, University of Notre Dame, Notre Dame, Indiana 46556

Michael Giersig

Hahn-Meitner Institut, 14109 Berlin, Germany

Received: October 14, 1999; In Final Form: March 9, 2000

The γ-radiolytic reduction of Hg^{2+} in aqueous solution in the presence of 0.3 M 2-propanol first leads to Hg_2^{2+} ($\epsilon_{237\ nm} = 3.2 \times 10^4\ M^{-1}\ cm^{-1}$), and later to colloidal mercury. When the reduction is carried out in the presence of colloidal gold nanoparticles, Hg_2^{2+} does not appear as an intermediate, and Hg_2^{2+} formed in the absence of gold does not react with added gold colloid. These effects are understood in terms of the reaction of a precursor, Hg^+, with the gold particles. The optical absorption spectra of the resulting mercury containing gold particles are reported for various Au/Hg ratios. The plasmon absorption band of gold is blue-shifted and damped, and a broad absorption band develops around 360 nm with increasing mercury content. The mercury of the composite particles is slowly reoxidized upon exposure of the solution to air. Excess Hg^{2+} ions in solution extract adsorbed mercury in the form of Hg_2^{2+}. Both the absorption spectra and electron micrographs of the gold particles are interpreted by a rather weak penetration of mercury into the particles and formation of a rather labile mercury layer around them.

Introduction

Mercury containing colloids have been very little investigated. In the early days of colloid science, amalgam colloids of Au, Ag, and Cu were prepared,[1,2,3] and, more recently, mercury containing silver colloids have been described.[4,5,6] The first amalgam colloids were made by mixing gold and mercury hydrosols, or by shaking a gold sol in contact with liquid mercury for a long time, and the chemical analysis showed that a complete interpenetration according to the molar Au/Hg ratio in solution had taken place.[1−3] Radiolytic reduction of Hg^{2+} in silver sols[4] and silmultaneous reduction of Ag^+ and Hg^{2+} ions by $NaBH_4$[5] or by radiation[6] was applied in the more recent work.

The renewed interest in such materials stems from the fact that mercury nanoparticles, like the above noble metals, have an intense plasmon absorption band; such bands are affected by a strong laser femto-flash with short relaxation times, thus making nanoparticles of metals a possible candidate in fast optical devices. The optical changes include signals from hot electron formation (electron−phonon coupling within some 100 fs) and acoustic quantum beats (within some 10 ps). We have recently described such effects on gold particles.[7] One of the goals of the present work was the preparation of gold−mercury particles suitable for such investigations. The results will be reported elsewhere.

In the present paper, the preparation and a few properties of such particles is described. Mercury is radiolytically deposited on 46 nm gold particles, and the mechanism of this deposition is discussed. The absorption spectra and electron micrographs of Au/Hg particles of different composition are reported.

Experimental Section

Au/Hg particles were synthesized in two steps. First, 46 nm gold particles were radiolytically prepared as described previously.[8] In this method, 23 nm particles from the standard reduction of $AuCl_3^-$ by citrate[9] were enlarged by a factor of 2. This enlargement consists of the reduction of the monovalent gold in added $Au(CN)_2^-$ by radiolytically generated free radicals directly on the surface of the gold seed particles, and subsequent removal of CN^- ions by ion-exchange resin. The deposition of mercury on the 46 nm gold particles was performed by adding $Hg(ClO_4)_2$ and 2-propanol to the gold sol, and then producing reducing free radicals by γ-irradiation. The reducing radicals are formed in the following processes:

primary radical formation from the aqueous solvent:

$$H_2O \rightarrow e_{aq}^-,\ \cdot H,\ \cdot OH \qquad (1)$$

radical attack on 2-propanol present at 0.3 M:

$$\cdot OH(\cdot H) + (CH_3)_2CHOH \rightarrow (CH_3)_2\cdot C(OH) + H_2O(H_2) \qquad (2)$$

Both the hydrated electron and the 1-hydroxyalkyl radical are able to rapidly reduce mercury ions. The reduced mercury species finally are deposited on the gold particles.

The solutions were irradiated in glass vessels, using commercial ^{60}Co γ-irradiation sources. The solutions were deaerated

* To whom correspondence should be addressed.

10.1021/jp993682p CCC: $19.00
Published on Web 05/04/2000

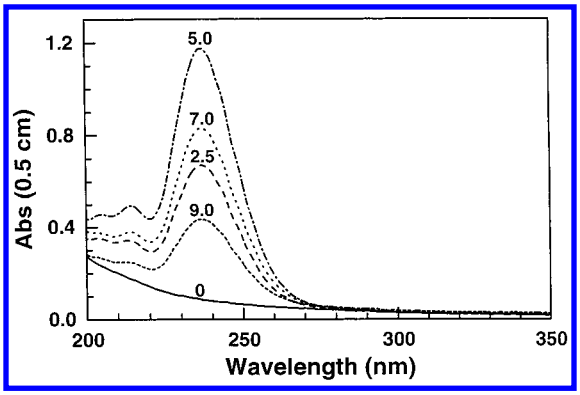

Figure 1. Absorption spectrum of a solution containing 2.0×10^{-4} M $Hg(ClO_4)_2$ and 0.3 M 2-propanol at various times (in minutes) of γ-irradiation. Dose rate: 2.6×10^5 rad/h.

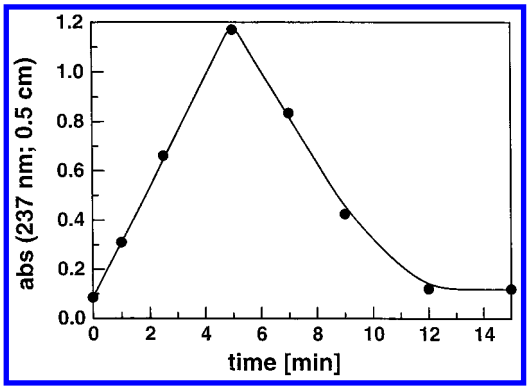

Figure 2. Absorbance at 237 nm as a function of irradiation time. Solution and dose rate as in Figure 1.

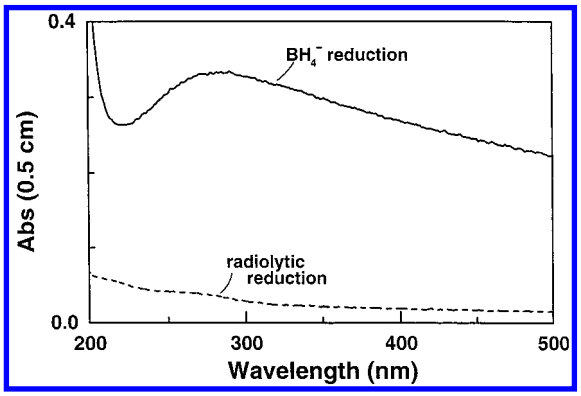

Figure 3. Absorption spectra after reduction of a 2.0×10^{-4} $Hg(ClO_4)_2$ solution by borohydride or γ-irradiation. Absence of colloidal gold.

by bubbling with pure argon prior to irradiation; the vessels were closed during irradiation. They contained sidearms carrying an optical cuvette and a septum; spectra could therefore be measured and substances added via syringe without exposure of the solutions to air. The optical path of the cuvette is indicated on the ordinate axis in the following absorption spectra. Electron microscopy was performed using a Philips 12 apparatus, 120 kV. Samples were prepared in an oxygen-free glovebox by putting a copper−carbon grid on a drop of the solution and letting the drop dry.

Results and Discussion

Reduction in the Absence of Gold Particles. A 2.0×10^{-4} M $Hg(ClO_4)_2$ solution, which also contained 0.3 M 2-propanol, was γ-irradiated and the optical absorption spectrum recorded at various irradiation times. The pH was 3.7. Divalent mercury is partly hydroxylated under these conditions. As can be seen from Figure 1, the 237 nm absorption band of Hg_2^{2+} builds up initially, and then decreases at longer irradiation times. In addition, the solution became slightly turbid. The turbidity is attributed to a tiny amount of colloidal mercury present in the equilibrium:

$$Hg_2^{2+} \rightleftarrows Hg_m + Hg^{2+} \quad (3)$$

(m: metal). In Figure 2, the 237 nm absorption is shown as a function of the irradiation time. Its build-up is attributed to the reactions:

$$e_{aq}^- ((CH_3)_2\cdot C(OH)) + HgOH^+ \rightarrow Hg^+ + OH^- (Hg^+ + (CH_3)_2CO + H_2O) \quad (4)$$

$$Hg^+ + Hg^+ \rightarrow Hg_2^{2+} \quad (5)$$

The optical absorption of Hg^+ has been detected in pulse radiolysis experiments.[10,11] At irradiation times longer than 5 min, the 237 nm absorption in Figure 2 decreases. As more and more Hg_2^{2+} is accumulated in the solution, its reduction,

$$Hg_2^{2+} + 2e^- \rightarrow 2\,Hg^0 \quad (6)$$

where e^- is an electron transferred from either e_{aq}^- or an organic radical becomes noticible. When about 50% of the divalent mercury has been consumed, reactions 6 become faster than reactions 4, and the Hg_2^{2+} concentration decreases with increasing irradiation time. From the initial slope of the 237 nm curve in Figure 2, and using a yield of 6.0 reducing radicals per 100 eV absorbed radiation energy, one calculates an absorption coefficient of Hg_2^{2+} of 3.2×10^4 M^{-1} cm^{-1}.

At the end of reduction (about 12 min in Figure 2), the solution exhibits a slight whitish opalescence. As can be seen from Figure 3, it has a very weak absorption over the whole range of the visible and UV without showing the plasmon maximum that is expected at 280 nm.[12] When 10^{-3} M sodium borohydride was added, no optical changes took place, which shows that the reduction had indeed been complete. Upon aging of the γ-irradiated solution, tiny mercury drops sedimented within 2 days.

Figure 3 also shows the spectrum that is observed, when the reduction of mercury is carried out using sodium borohydride. Under these circumstances, a brown and strongly opalescent solution is immediately obtained, whose spectrum exhibits a broad maximum at the expected wavelength of 280 nm; particles, or better, drops of mercury, with diameters around 100 nm are present.[5] The differences in the spectra of colloidal mercury of Figure 3 are remarkable; they must result from the very different rates in the two reductions. In the radiolytic reduction, mercury is very slowly formed. This seems to lead to rather large drops, whose refractive index is close to that of the aqueous solvent.

Reduction in the Presence of Gold Particles. The experiment of Figure 1 was repeated with a solution, which contained 3.2×10^{-4} M colloidal gold in addition to the components in Figure 1. Under these conditions, $HgOH^+$ is attacked by the free radicals as in the absence of gold particles, the reason being that the hydrated electrons and organic radicals cannot reach the nanoparticles because of the very low concentration of the latter (at a particle size of 46 nm and an overall gold concentration of 3.2×10^{-4} M, one calculates a particle concentration of 10^{-10} M). However, contrary to what was

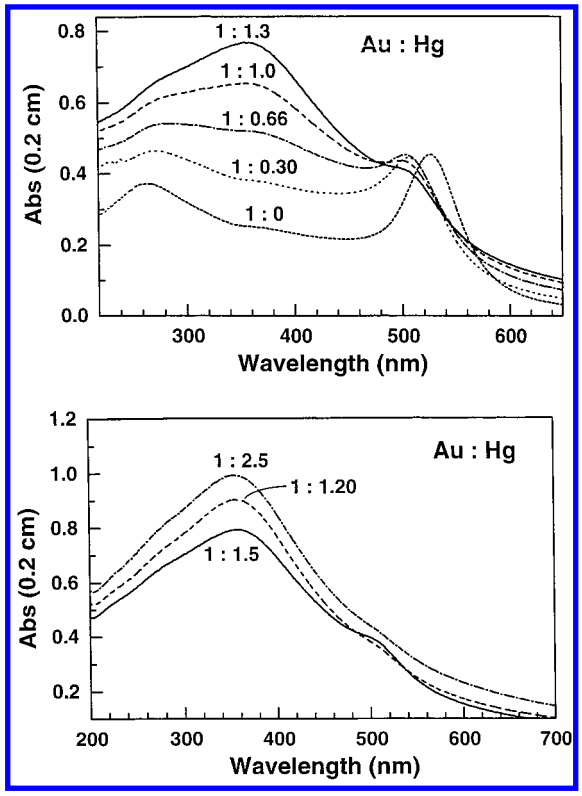

Figure 4. (a) Absorption spectrum of the original colloidal gold particles, and after deposition of various amounts of mercury. Overall gold concentration: 3.2×10^{-4} M. Dose rate: 8.5×10^4 rad/h. The molar Au/Hg ratio is given on the curves. (b) Absorption spectra as in Figure 4a at higher mercury depositions.

observed in the absence of gold (Figures 1 and 2), the absorption of Hg_2^{2+} at 237 nm was not built up in the early stages of irradiation.

Moreover, the solution did not become opalescent, and there was no sedimentation of mercury after several days. The absorption spectrum of the gold particles changed significantly as shown by Figures 4 a and b. In these experiments, different $Hg(ClO_4)_2$ concentrations were used, and the irradiation continued until all the mercury was reduced; this point was recognized when further irradiation did not lead to additional optical changes. The spectra in Figures 4 do not constitute a superposition of the spectrum of pure gold (Figure 4a, 1:0) and that of pure mercury (Figure 3, lower curve). All these observations point to some kind of deposition of reduced mercury on the gold particles. The red color of the gold solution became more and more orange-brown with increasing mercury deposition.

One could be tempted by the absence of Hg_2^{2+} as a product to ascribe the mercury deposition to a reaction of Hg_2^{2+} with the gold particles, assuming that Hg_2^{2+} was initially formed as in the absence of gold. However, the following experiment shows that Hg_2^{2+} is not reactive toward nano gold particles. A solution of Hg_2^{2+} was made as in Figure 2 (5 min irradiation), and then mixed under exclusion of air with an equal volume of the gold sol. The mixed solution was stable for days and did not exhibit any decrease in the 237 nm absorption band of Hg_2^{2+} or any change in the absorption spectrum of the gold particles. The conclusion is that Hg_2^{2+} is not formed in the initial stages of reduction when gold is present. This is understood if the precursor of Hg_2^{2+}, Hg^+, eq 5, reacts with the gold particles. For example, a gold catalyzed disproportionation of Hg^+ could occur,

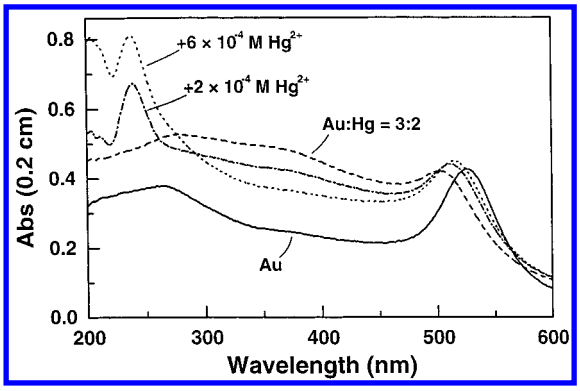

Figure 5. Absorption spectrum of the gold sol before (Au) and after (Au/Hg) deposition of mercury in the molar ratio 3:2, and the spectra after two additions of excess mercury perchlorate. All additions under exclusion of air.

$$x\,Hg^+ + Au_n \rightarrow Au_nHg_x^{x+} \quad (7)$$

$$Au_nHg_x^{x+} + Hg^+ \rightarrow Au_nHg_x^{(x-1)+} + Hg^{2+} \quad (8)$$

Stability of the Au−Hg Particles. When a solution of the composite particles was exposed to air, optical changes took place within hours and days: the red color of gold reappeared, and the plasmon absorption band of gold became more pronounced and red-shifted. Clearly, a slow oxidation of the mercury in the gold particles had occurred. A very much faster oxidation was observed, when excess Hg^{2+} was introduced into a solution of the composite particles. Figure 5 shows a typical experiment: The spectra of the pure gold particles and of the Au−Hg particles resulting from mercury deposition in the molar ratio 3:2 are shown. In addition, the figure contains the spectra which were recorded after the addition of 2 and 6 times 10^{-4} M mercury perchlorate. These additions cause the 237 nm band of Hg_2^{2+} to appear, and the gold plasmon band to red-shift in the 500 to 520 nm region. These effects are explained by the extraction of mercury atoms from the composite particles by Hg^{2+}:

$$Au_nHg_m + Hg^{2+} \rightarrow Au_nHg_{(m-1)} + Hg_2^{2+} \quad (9)$$

Absorption Spectra of Composite Au/Hg Particles. The pure gold colloid has a surface plasmon absorption band at 526 nm, and a band at 270 nm, which is caused by interband transitions. With increasing Hg deposition in Figure 4a and b, the plasmon band moves to shorter wavelengths and becomes weaker. The 270 nm gold absorption also is more strongly shielded, and a second broad absorption band builds up in the 300 to 400 nm range.

It is interesting to compare the above spectra with the spectra of silver colloids which carry different amounts of mercury. The Ag/Hg spectra are dominated by a single plasmon absorption band, which continuously shifts from 380 nm (pure silver) to 280 nm (pure mercury) and is sensitive to changes on the surface of the particles.[4,5] It has also been shown that an amalgam structure exists throughout the Ag/Hg particles.[4−6] The Au/Hg particles, on the other hand, exhibit a distinctly different behavior: The gold plasmon band is only slightly blue-shifted with increasing Hg content, and a new band at 360 nm builds up; the latter band becomes stronger without shifting to shorter wavelengths with increasing Hg content, i.e., does not exhibit a clear transition to the 280 nm band of pure Hg colloid. These differences to the spectra of Ag/Hg particles may be taken as an indication for a different structure of the Au/Hg particles,

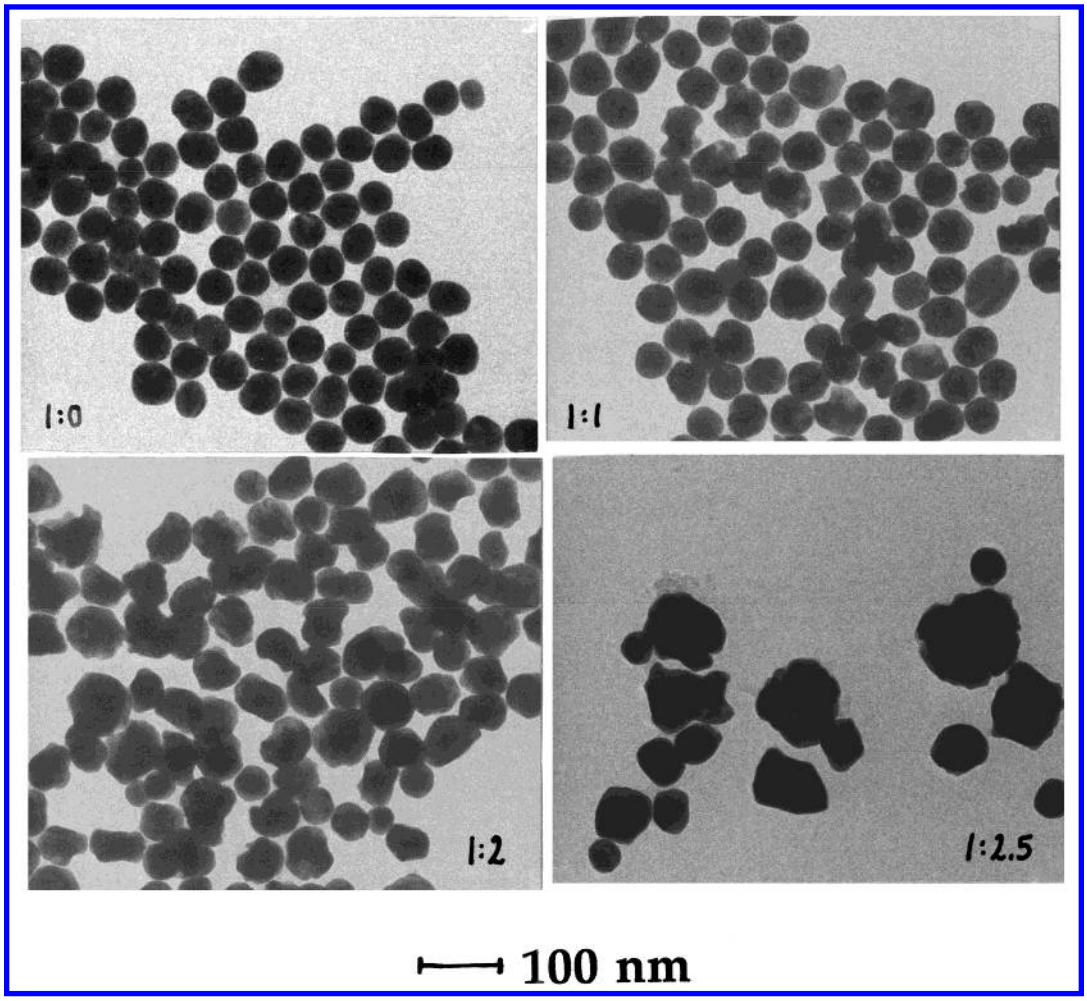

Figure 6. Electron micrographs: particles before and after deposition of mercury. The Au/Hg ratio is indicated.

such as a nonunifom distribution of mercury, i.e., a low Hg concentration in the interior, and a mercury-rich outer layer.

Electron Micrographs. Figure 6 shows electron micrographs of uncoated and Hg-coated gold particles. The uncoated particles are close to monodisperse (mean size: 46 nm; standard size deviation: 7%). Assuming that the deposited mercury has the same molar volume as liquid mercury, one calculates a ratio R of the radii of the coated to uncoated particles according to the relationship

$$R = \left(1 + \frac{V_{m,Hg}[Hg]}{V_{m,Au}[Au]}\right)^{1/3} \qquad (10)$$

where the V_m and the [ ] are the molar volumes and overall concentrations of the two metals, respectively. It was found that the ratio R is significantly smaller for all coated particles than expected from eq 10. For example, at an Au/Hg ratio of 1:0.5, $R = 1.09$ was found as compared to the theoretical value of 1.2. The energy-dispersive X-ray analysis yielded a molar ratio Au/Hg of only 91:9, and the electron micrograph shows particles with a 2 nm amorphous Hg layer, many of the particles being embedded in a mercury matrix. With increasing Hg content in Figure 6, the morphology of the particles changes, many nonspherical shapes are seen, pure mercury blobs appear, and coalescence of particles takes place to an increasing extent. Thus, the behavior of Au−Hg particles is quite different from that of Ag−Hg particles, which are completely amalgamated.[4−6]

These observations corroborate the conclusions drawn from the absorption spectra: Amalgamation of the gold particles takes place only to a very limited extent, most of the mercury being deposited as a layer around the particles. This layer is probably not a liquid, as it might be solidified by a small content of gold. The mercury can readily be expelled to a large extent from this layer; this possibly happens when the solution is dried on the grid (if the expulsion had already happened in solution, mercury metal should have sedimented from the solution). At this point it is also interesting to remember the technological process by which gold is extracted from ores by mercury;[13] the mercury, which is mainly physically attached to the gold, is removed from the amalgam formed by exposing the amalgam to a high pressure. It seems that expulsion of mercury from Hg-containing nanoparticles is particularly efficient; the reason for this effect is possibly the high surface pressure in such particles.

Acknowledgment. The authors thank Prof. D. Meisel for valuable discussions, and Mrs. U. Bloeck for technical assistence in the TEM experiments. We also thank Dr. Paul Mulvaney, University of Melbourne, for communicating to us calculated spectra of both pure Hg and $Au_{core}Hg_{shell}$ nanoparticles; these spectra agree within 20% with the experimental spectra in Figure 4a and b, which strongly corroborates the above conclusions. The work described herein was supported by the Office of Basic Energy Sciences of the U.S. Department of Energy. This is Contribution No. 4165 NDRL from the Notre Dame Radiation Laboratory.

References and Notes

(1) Amberger, K. *Kolloid-Z.* **1911**, *8*, 88.
(2) Paal, C.; Steyer, H. *Kolloid-Z.* **1918**, *23*, 10.

(3) Paal, C.; Steyer, H. *Kolloid-Z.* **1919**, *25*, 21.
(4) Katsikas, L.; Gutiérrez, M.; Henglein, A. *J. Phys. Chem.* **1996**, *100*, 11 203.
(5) Henglein, A.; Brancewicz, C. *Chem. Mater.* **1997**, *9*, 2164.
(6) Su, D.; Katsikas, L.; Giersig, M. *Ber. Bunsen-Ges. Phys. Chem.* **1997**, *101*, 1644.
(7) (a) Hodak, J.; Martini, I.; Hartland, G. V. *Chem. Phys. Lett.* **1998**, *284*, 15. (b) Hodak, J.; Martini, I.; Hartland, G. V. *J. Chem. Phys.* **1998**, *108*, 9210. (c) Hodak, J.; Henglein, A.; Hartland, G. V. *J. Chem. Phys.* **1999**, *111*, 8613. (d) Hodak, J. H.; Henglein, A.; Hartland, G. V. *J. Chem. Phys.* **2000**, *112*, 5942.
(8) (a) Henglein, A.; Meisel, D. *Langmuir* **1998**, *102*, 8364. (b) Henglein, *Langmuir* **1999**, *15*, 6738.
(9) Enüstün, B. V.; Turkevich, J. *J. Am. Chem. Soc.* **1963**, *85*, 317.
(10) Faraggi, M.; Amozig, A. *Int. J. Radiat. Phys. Chem.* **1972**, *4*, 353.
(11) Fujita, S.; Horii, H.; Taniguchi, S. *J. Phys. Chem.* **1973**, *77*, 2868.
(12) Creighton, J. A.; Eadon, D. G. *J. Chem. Soc., Faraday Trans.* **1991**, *87*, 3881.
(13) (a) Gmelins Handbuch der Anorganischen Chemie, 8. Auflage, Nr. 62, Verlag Chemie: Weinheim, l952, p 289. (b) Sneed, M. C.; Maynard, J. L.; Brasted, R. C. Comprehensive Inorganic Chemistry, Vol. 2, D. Van Nostrand Co., Inc.: New York, 1954; p. 100.